

Critical Review of Basic Afterglow Concepts

Jonathan Granot ^{a,b}

^a*Kavli Institute for Particle Astrophysics and Cosmology, Stanford University,
P.O. Box 20450, MS 29, Stanford, CA 94309, USA*

^b*Centre for Astrophysics Research, University of Hertfordshire, College Lane,
Hatfield, Herts, AL10 9AB, UK*

Abstract

The long lived afterglow emission that follows gamma-ray bursts (GRBs) was predicted prior to its detection in 1997, in the X-rays, optical and radio. It is thought to arise from the shock that is driven into the external medium as the latter decelerates the relativistic outflow that drives the GRB, and persists well after most of the energy in the outflow is transferred to the shocked external medium. As the blast wave decelerates, the typical emission frequency shifts to longer wavelength. Recent observations following the launch of the *Swift* satellite challenge the traditional afterglow modeling and call into questions some of the basic underlying concepts. This brief review outlines some of the major strengths and weaknesses of the standard afterglow model, as well as some of the challenges that it faces in explaining recent data, and potential directions for future study that may eventually help overcome some of the current difficulties.

Key words: gamma-rays: bursts

PACS: 98.70.Rz

1 Introduction

Gamma-ray bursts (GRBs) are thought to originate from an ultra-relativistic outflow that is driven by a sudden catastrophic energy re-

lease from a compact stellar central source. The prompt γ -ray emission is usually attributed to energy dissipation within the relativistic outflow. The outflow sweeps up the external medium and drives a strong relativistic shock into it, until the outflow is eventually decelerated significantly and most of the energy in the flow is transferred to the shocked external medium (for recent reviews see Piran, 2005; Mészáros, 2006). The shocked external medium is thought to produce the long lived afterglow

Email address:

j.granot@herts.ac.uk (Jonathan Granot).

URL:

<http://star.herts.ac.uk/~granot> (Jonathan Granot).

emission that is detected in the X-rays, optical, and radio for days, weeks, and months, respectively, after the GRB.

Afterglow emission was predicted (Paczynski & Rhoads, 1993; Katz, 1994; Mészáros & Rees, 1997; Sari & Pirani, 1997) prior to its detection in 1997 in the X-ray (Costa et al., 1997), optical (van Paradijs et al., 1997), and radio (Frail et al., 1997). Furthermore, its basic observational properties (light curve and spectrum) initially agreed rather well with the simple model predictions (Waxman, 1997; Wijers, Rees & Mészáros, 1997). This gave some credence to the basic picture where the afterglow emission arises from the external shock going into the ambient medium, where the typical emission frequency gradually shifts to longer wavelength as the blast wave decelerates.

As afterglow observations improved, however, new and more complicated behavior was observed, which could not be accommodated by the simplest version of the external shock afterglow model (which features a spherical adiabatic blast wave propagating into a uniform external medium). This called for new ingredients in the model, i.e. variants of the simplest model. Some of these variants and their observational signatures were predicted before they were observed, which again provided support for the basic model.

The Launch of the *Swift* satellite in November 2004 marked a new era in GRB research. Its ability to rapidly and autonomously slew to the di-

rection of GRBs that it detects and observe them in the X-rays, UV, and optical has significantly improved our knowledge of the early afterglow, from tens of seconds to hours after the onset of the GRB. The complex behavior that was revealed challenges the traditional afterglow theory, and even puts to question the basic underlying picture.

In § 2 a short overview is given of the standard afterglow model, starting from the dynamics in the simplest case (§ 2.1), continuing with the emission mechanism (§ 2.2), and finishing with variants of the simplest model (§ 2.3). Next, § 3 outlines some of the weaknesses of the standard afterglow model. In § 4 a brief description is given of the major new observations in the *Swift* era, stressing the difficulties and challenges that they present for the standard afterglow model. Finally, § 5 describes the crisis for afterglow theory that was caused by the new observations, and discusses some ideas for resolving the crisis as well as possible directions for the future.

2 Brief Overview of Standard Afterglow Theory

2.1 The Simplest Hydrodynamic Model: a “Spherical Cow”

The simplest version of the standard afterglow model features a spherical relativistic adiabatic (with negligible energy losses or gains) blast wave that propagates into a uniform external medium, of mass density

$\rho_{\text{ext}} = n_{\text{ext}} m_p$. Initially, the outflow is decelerated by a reverse shock¹, while the external medium is swept-up by the forward shock, where the two shocked regions are separated by a contact discontinuity. The ejecta are decelerated by the reverse shock from their original Lorentz factor, Γ_{ej} , to a smaller Lorentz factor, η , where $\Gamma_{\text{ej}} > \eta \gg 1$.

If $\Gamma_{\text{ej}}^2 \rho_{\text{ext}} / \rho_{\text{ej}} \gg 1$, where ρ_{ej} and ρ_{ext} are the proper mass densities (more generally, one should use the ratio of enthalpy densities) of the original ejecta and the external medium, respectively, then the reverse shock is relativistic. In this case the relative Lorentz factor between the upstream and downstream fluids across the reverse shock, $\Gamma_{\text{RS}} \approx (\Gamma_{\text{ej}}/\eta + \eta/\Gamma_{\text{ej}})/2$, is given by $\Gamma_{\text{RS}} \approx (\Gamma_{\text{ej}}/2)^{1/2} (\rho_{\text{ext}}/\rho_{\text{ej}})^{1/4} \gg 1$. If $\Gamma_{\text{ej}}^2 \rho_{\text{ext}} / \rho_{\text{ej}} \ll 1$ then the reverse shock is Newtonian and $\eta \approx \Gamma_{\text{ej}}$ while $\Gamma_{\text{RS}} - 1 \approx (4/7) \Gamma_{\text{ej}}^2 (\rho_{\text{ext}}/\rho_{\text{ej}}) \ll 1$ (Sari & Piran, 1995). This basic result may be obtained by equating the ram pressure (momentum flux) of the incoming fluids (ejecta and external medium) in the rest frame of the shocked fluids, $\rho_{\text{ej}}(\Gamma_{\text{RS}}^2 - 1) \approx \rho_{\text{ext}}\eta^2$.

If the reverse shock is initially Newtonian, then a reasonable spread in the Lorentz factor of the outflow ($\Delta\Gamma_{\text{ej}} \sim \Gamma_{\text{ej}}$) would cause the reverse shock to

strengthen more rapidly as it crosses the ejecta shell (since the shell starts to spread in the radial direction causing a faster drop in its density) in such a way that it becomes mildly relativistic when the reverse shock finishes crossing the shell. Therefore, in this case as well (as for an initially relativistic reverse shock), most of the energy is transferred to the shocked external medium within a single shell crossing by the reverse shock.

A bright optical emission, referred to as an ‘‘optical flash’’ was predicted from the reverse shock on a time scale similar to that of the prompt GRB emission (Sari & Piran, 1999a). Soon thereafter it was observed in GRB 990123 (Akerlof et al., 1999) and found to be in good agreement with the theoretical expectations (Sari & Piran, 1999b; Mészáros & Rees, 1999, see Figure 1). It was also supported by the detection of a ‘‘radio flare’’ (Kulkarni et al., 1999), which was attributed to the emission from the shocked ejecta well after the passage of the reverse shock, as its electrons cool adiabatically at the back of the self-similar hydrodynamic profile and their typical emission frequency passes through the radio after a day or so. This was considered another success of what has by then become the standard afterglow model.

After the initial stage in which the original outflow is significantly decelerated, most of the energy is given to the shocked external medium and the flow becomes self-similar (Blandford & McKee, 1976). The deceleration epoch ends and the self-

¹ The shocked outflow as a whole is further decelerated by work that is performed on it by the shocked external medium across the contact discontinuity that separates them, while each of its fluid elements is decelerated by the pressure gradients that form within it.

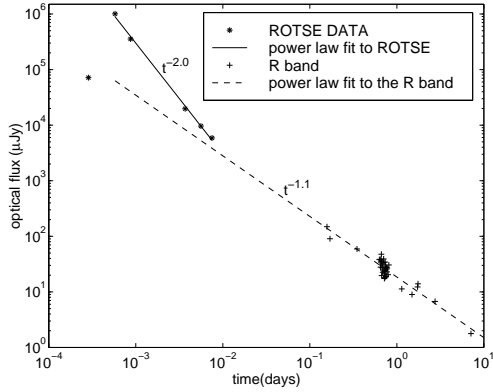


Fig. 1. Optical light curve of GRB 990123, where the early Robotic Optical Transient Search Experiment (ROTSE) measurements (the “optical flash”), excluding the first one, and the later R-band data are each described by a different power law, and attributed to the reverse shock and to the forward shock, respectively (from Sari & Piran, 1999b).

similar stage starts at a radius $R_{\text{dec}} \approx (3E/4\pi\rho_{\text{ext}}c^2\eta^2)^{1/3}$ and an observed time $t_{\text{dec}} \approx R_{\text{dec}}/2c\eta^2$, where $\eta \approx \min[\Gamma_{\text{ej}}, (\Gamma_{\text{ej}}/2)^{1/2}(\rho_{\text{ej}}/\rho_{\text{ext}})^{1/4}]$. During the relativistic self-similar stage, the Lorentz factor Γ of the shocked external medium scales as a power law with radius R . The scaling is easy to understand if one keeps in mind that in the (downstream) rest frame of the shocked fluid the cold upstream fluid comes in with a bulk Lorentz factor of Γ , and at the shock front this ordered bulk motion turns into random motion with the same average Lorentz factor. In the lab frame the average energy per particle is larger roughly by a factor of Γ compared to the downstream rest frame of the shocked fluid, and therefore $E \approx \Gamma^2 Mc^2$ where M is the total amount of swept-up (rest) mass. For a Uniform

medium $M \propto R^3$ and therefore for an adiabatic blast wave (for which $E \approx \text{const}$) $\Gamma = \eta(R/R_{\text{dec}})^{-3/2}$ since $\eta = \Gamma(R_{\text{dec}})$. The relativistic self-similar stage ends at $t_{\text{NR}} \approx (3E/4\pi\rho_{\text{ext}}c^5)^{1/3} \sim \eta^{8/3}t_{\text{dec}}$ when the flow becomes non-relativistic, after which it approaches the Newtonian Sedov-Taylor solution.

2.2 Emission Mechanism

The dominant emission mechanism in the afterglow is thought to be synchrotron radiation, of shock-accelerated relativistic electrons that gyrate in the post-shock magnetic fields. This is supported by the broad band afterglow spectrum, which consists of several power law segments (e.g., Galama et al., 1998, see Figure 2), and by the detection of linear polarization at the level of a few percent in the optical or NIR afterglows of several GRBs (Covino et al., 1999; Wijers et al., 1999; Rol et al., 2000; Covino et al., 2003). Synchrotron self-Compton (SSC; the inverse-Compton scattering of the synchrotron photons by the same population of relativistic electrons that emits the synchrotron photons) can sometimes dominate the afterglow flux in the X-rays (Sari & Esin, 2001; Harrison et al., 2001). The power-law nature of the broad band spectrum suggests a power law energy distribution of shock-accelerated electrons.

The electrons and magnetic fields behind the shock are assumed to hold some fixed fractions (ϵ_e and

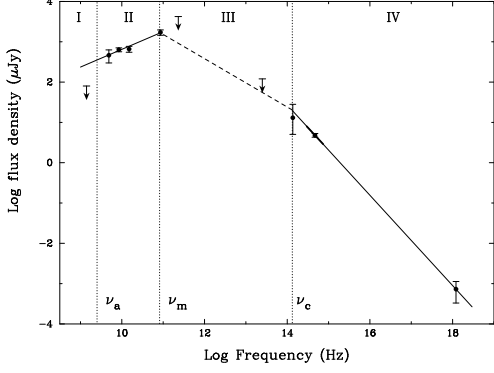


Fig. 2. The X-ray to radio afterglow spectrum of GRB 970508 at 12.1 days after the GRB (from Galama et al., 1998). A fit to the low-frequency part (4.86 – 86 GHz) with $F_\nu \propto \nu^{0.44 \pm 0.07}$ is shown as well as the extrapolation from X-ray to optical (*solid lines*). The local optical spectral slope (2.1 – 5.0 days after the event) is indicated by the thick solid line. Also indicated is the extrapolation $F_\nu \propto \nu^{-0.6}$ (*dashed line*). Indicated are the rough estimates of the break frequencies ν_a (due to self-absorption), ν_m (typical synchrotron frequency) and ν_c (due to electron cooling).

ϵ_B , respectively) of the internal energy. This reproduces the observed spectrum rather well, while together with the simple spherical self-similar dynamics outlined above, it predicts light curves which also consist of several power law segments. A change in the temporal index occurs either when a spectral break frequency sweeps past the observed frequency (in which case it is accompanied by a change in the spectral slope near the observed frequency), or when a hydrodynamic transition occurs (in which case no change in the spectral slope is expected across the temporal break). Figure 3 shows the various options for the broad band spectrum, as well as the temporal scaling of

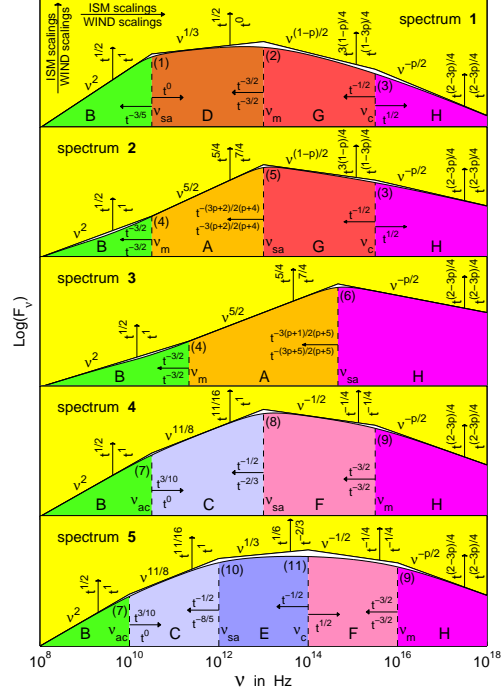


Fig. 3. The afterglow synchrotron spectrum, calculated for the Blandford & McKee (1976) spherical self-similar solution, under standard assumptions, using the accurate form of the synchrotron spectral emissivity and integration over the emission from the whole volume of shocked material behind the forward (afterglow) shock (for details see Granot & Sari, 2002). The different panels show the possible broad band spectra of the afterglow synchrotron emission, each corresponding to a different ordering of the spectral break frequencies.

the flux within each of the different power law segments of the spectrum for a spherical adiabatic blast wave given by the Blandford & McKee (1976) self-similar solution, for either a uniform external medium, or a wind-like external density profile (which is discussed in § 2.3).

2.3 Variants of the Basic Model

Several variations on the simplest model have been discussed in the literature, as well as their observational signatures, many of which were proposed before their observational manifestations were detected. Radiative losses have been considered (Blandford & McKee, 1976; Cohen, Piran & Sari, 1998; Böttcher & Dermer, 2000), and result in a faster decrease of the Lorentz factor with radius, since $\Gamma^2 \approx E(R)/M(R)c^2$, and also with the observed time. This, in turn, together with the decrease in time of the energy in the afterglow shock result in a faster decay of the optical and X-ray fluxes. Conversely, energy injection into the afterglow shock (e.g., Sari & Mészáros, 2000), would result in a slower flux decay.

A general power law index for the external density, $\rho_{\text{ext}} = Ar^{-k}$ with $k < 3$ was considered early on (Blandford & McKee, 1976). It was only much later, however, when a specific theoretical motivation for such a non-uniform external density profile in the context of GRBs was pointed out (Chevalier & Li, 1999), as evidence accumulated in favor of a massive star progenitor that is expected to be surrounded by its pre-supernova stellar wind with $k \approx 2$. A steeper external density profile (larger k) results in a faster flux decay in the optical (and also in X-rays, if below the cooling frequency ν_c).

It has also been realized that, similar to other astrophysical sources

of relativistic outflow such as active galactic nuclei and micro-quasars, the GRB outflow is also expected to be collimated into narrow bipolar jets (e.g., Rhoads, 1997). This idea became even more compelling as the measured redshifts of several GRBs, which became available thanks to the detection of their afterglows, implied very large energy output in γ -rays assuming isotropic emission, $E_{\gamma,\text{iso}}$, which approached and in one case (GRB 991023) even exceeded a solar rest energy. If most of the γ -rays are emitted within a small fraction, $f_b \ll 1$, of the total solid angle (where $f_b \approx \theta_0^2/2$ for conical uniform narrow bipolar jets of initial half-opening angle θ_0), then the true energy output in γ -rays, E_γ , is much smaller than its isotropic equivalent value, $E_\gamma = f_b E_{\gamma,\text{iso}}$.

Simple semi-analytic models for uniform conical jets which expand sideways rapidly when their Lorentz factor Γ drops below θ_0^{-1} predicted an achromatic steepening of the afterglow flux decay, i.e. a “jet break” in the afterglow light curve (Rhoads, 1997, 1999; Sari, Piran & Halpern, 1999). Such jet breaks in the afterglow light curves of many GRBs were indeed detected soon thereafter (an example is shown in Figure 4), which provided good support for GRB outflows being collimated into narrow jets. The structure and dynamics of GRB jets, however, are still not fully explored (for a recent review see Granot, 2007a).

In the pre-*Swift* era, while most afterglow light curves showed a smooth power law decay (Stanek et al.,

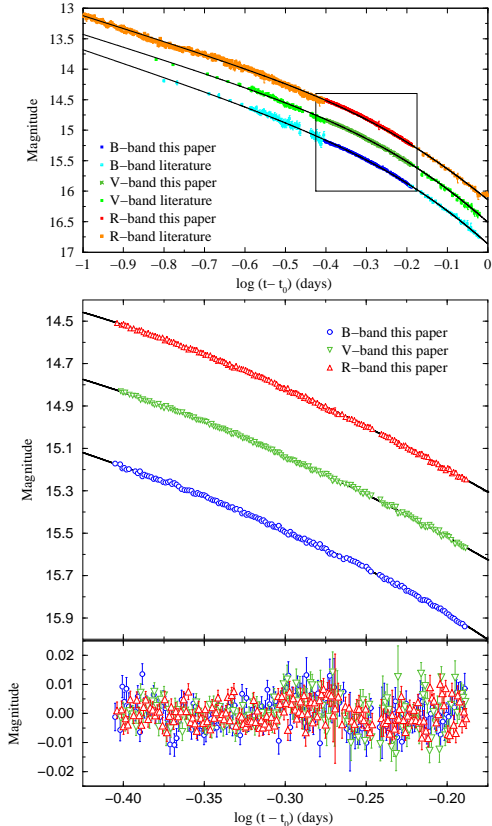


Fig. 4. Optical light curves at three different frequencies (BVR -bands) of the GRB 030329, which show a clear achromatic break, attributed to a jet, and are fitted to a model featuring two power laws that join smoothly at the jet break time (from Gorosabel et al., 2006). The bottom panel shows the fit residuals.

1999; Laursen, & Stanek, 2003; Gorosabel et al., 2006), and sometimes also a “jet break”, some optical afterglows have shown significant temporal variability, with strong deviations from the more typical smooth power law behavior. The best examples are GRBs 021004 (Pandey et al., 2002; Fox et al., 2003; Bersier et al., 2003) and 030329 (Lipkin et al., 2004). Possible variants of the simplest standard afterglow model have been suggested in order to account for such tem-

poral variability in GRB afterglow light curves. These include variations in the external density (e.g., Wang & Loeb, 2000; Lazzati et al., 2002; Nakar, Piran & Granot, 2003; Nakar & Piran, 2003, see, however, Nakar & Granot 2007), or in the energy of the afterglow shock. The latter includes energy injection by “refreshed shocks” – slower shells of ejecta that catch up with the afterglow shock on long time scales (e.g., Rees & Mészáros, 1998; Kumar & Piran, 2000a; Sari & Mészáros, 2000; Ramirez-Ruiz, Merloni & Rees, 2001; Granot, Nakar & Piran, 2003) or a “patchy shell” – angular inhomogeneities within the outflow (e.g., Kumar & Piran, 2000b; Nakar, Piran & Granot, 2003; Heyl & Perna, 2003; Nakar & Oren, 2004). Another possible cause for variability in the afterglow light curve, although it is expected to be quite rare, is microlensing by an intervening star in a galaxy that happens to be close to our line of sight (Garnavich, Loeb & Stanek, 2000; Gaudi, Granot & Loeb, 2001).

Finally, it is worth mentioning another success of the standard afterglow model: the prediction for the size of the afterglow image which agrees very well with the available observations. For GRB 970508 an estimate of the image size of $\sim 10^{17}$ cm after ~ 30 days was obtained from the quenching of diffractive scintillations in the radio (Frail et al., 1997; Waxman, Kulkarni & Frail, 1998). For GRB 030329 the size of the afterglow image was measured directly by radio interferometry with the VLBA at several different epochs (Taylor et al.,

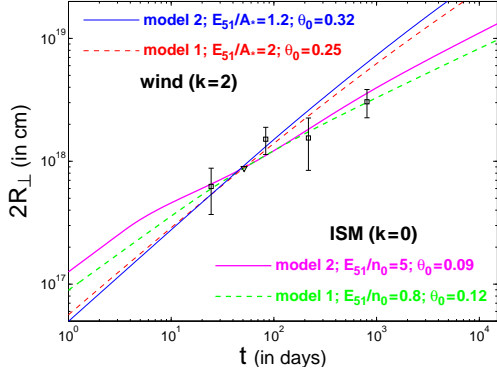


Fig. 5. Tentative fits of theoretical models for the evolution of the source size (from Granot, Ramirez-Ruiz & Loeb, 2005) to the observed image size (of diameter $2R_{\perp}$) of the radio afterglow of GRB 030329 (from Pihlström et al., 2007). In model 1 there is relativistic lateral spreading of the GRB jet in its local rest frame, while in model 2 there is no significant lateral expansion until the jet becomes non-relativistic. The external density is taken to be a power law with the distance r from the source, $\rho_{\text{ext}} = Ar^{-k}$, where $k = 0$ for a uniform external density while $k = 2$ is expected for a stellar wind environment.

2004, 2005; Pihlström et al., 2007) and agrees well with the expectations of the standard afterglow model (Oren, Nakar & Piran, 2004; Granot, Ramirez-Ruiz & Loeb, 2005), as illustrated in Figure 5.

3 Some Weaknesses of the Standard Afterglow Model

Despite its many successes, the standard afterglow model has several weaknesses, two of which we briefly mention here.

The study of the physics of relativistic collisionless shocks is still

at its infancy, and the standard afterglow model simply parameterizes our ignorance. The usual assumptions are that (i) the magnetic field everywhere within the shocked region holds a constant fraction, ϵ_B , of the internal energy, and (ii) just behind the shock front all electrons are accelerated into a power law energy distribution (of index p) with a sharp low energy cutoff and hold a fixed fraction, ϵ_e , of the internal energy. The validity of these assumptions is not clear, and they are not fully supported by first principles calculations. In principle, even if the electron energy distribution may be reasonably approximated as a power law, the parameters ϵ_e and p may vary with the shock Lorentz factor and the upstream composition. The same holds for ϵ_B , which may also vary (decrease) with the distance behind the shock. Moreover, likely only some fraction $\xi_e < 1$ of the electrons are accelerated into a power-law distribution of energies (the rest forming a quasi-thermal population).

This is an active field of research, with a lot of recent progress involving both analytic work (e.g., Medvedev & Loeb, 1999; Kesht & Waxman, 2005; Lyubarsky & Eichler, 2006) and particle in cell numerical simulations (e.g., Spitkovsky, 2007, and references therein). Nevertheless, the major questions are still not fully resolved. These include the decay of the magnetic field downstream of the shock transition and whether it saturates at some finite value that can explain afterglow observations within the standard picture, how particles are acceleration in these shocks and

to what energy distribution.

The dynamics of GRB jets as they sweep-up the external medium, decelerate, and eventually expand sideways, have still not been studied in much detail, despite the important implications for GRB afterglows and GRB physics in general (for a recent review see Granot, 2007a). While simple semi-analytic models suggest that after Γ drops below θ_0^{-1} the jet starts expanding laterally exponentially with radius (Rhoads, 1999; Sari, Piran & Halpern, 1999), numerical simulations show a much more modest degree of lateral expansion where most of the energy in the flow remains within the original opening angle as long as the jet is relativistic (Granot et al., 2001; Kumar & Granot, 2003; Cannizzo et al., 2004). Recently, a self-similar solution has been found (Gruzinov, 2007) in the lines of the simple semi-analytic models. However, it appears to be approached very slowly, so that for realistic initial conditions it may not be fully applicable and the lateral expansion may indeed be very modest.

4 The *Swift* Era: New Observations and their Implications

Swift has discovered surprising new features in the early X-ray afterglow (Nousek et al., 2006). These included mainly (i) an initial rapid decay phase where $F_\nu \propto t^{-\alpha}$ with $3 \lesssim \alpha_1 \lesssim 5$ lasting from the end of the prompt emission up to $\sim 10^{2.5}$ s, (ii) a subsequent shallow decay phase

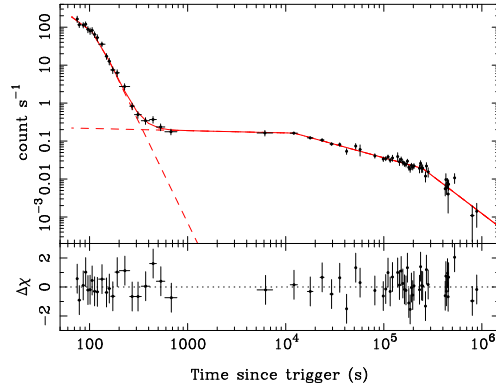


Fig. 6. Light curve of GRB 050315 in the 0.2 – 5 keV band, taken by the *Swift* X-ray telescope (XRT), also showing the best-fitting model comprising a singly broken power law and a double broken power law, which dominate at early and late times, respectively (from Vaughan et al., 2006). The lower panel shows the residuals of the fit.

where $0.2 \lesssim \alpha_2 \lesssim 0.8$, lasting up to $\sim 10^4$ s (followed by the familiar pre-*swift* power law decay with $1 \lesssim \alpha_3 \lesssim 1.5$), and (iii) X-ray flares, which appear to be overlaid on top of the underlying power law decay in stages (i) and (ii). A good example of such an X-ray light curve that shows these different stages (but no X-ray flares) as well as a possible jet break, is GRB 050315, which is shown in Figure 6. The initial rapid decay stage seems to be a smooth extension of the prompt emission (O’Brien et al., 2006), and is therefore most likely the tail of the prompt GRB, probably due to emission from large angles relative to our line of sight (Kumar & Panaitescu, 2000).

The X-ray flares appear to be a distinct emission component, as suggested by their generally different spectrum compared to the underlying power law component, and by the

fact that the flux after a flare is usually the continuation of the same underlying power law component from before the flare (e.g., Burrows et al., 2005). In many cases these flares show sharp large amplitude flux variation on time scales $\Delta t \ll t$ (see, e.g. Krimm et al., 2007), which are very hard to produce by the external shock, and suggest a sporadic late time activity of the central source. An alternative explanation, which does not require a prolonged central source activity, is delayed magnetic reconnection events in the outflow (Giannios 2006).

The shallow decay phase, stage (ii), and the initial rapid decay phase, stage (i), appear to arise from two physically distinct emission regions. This is supported by a change in the spectral index that is observed in some of the transitions between these two stages (Nousek et al., 2006). Furthermore, the shallow decay phase eventually smoothly steepens into the familiar pre-*Swift* flux decay, which is well established to be afterglow emission (that is attributed to the forward shock in the standard scenario), strongly suggesting that the shallow decay phase is similarly afterglow emission. This is also supported by the fact that there is no evidence for a change in the spectral index across this break (Nousek et al., 2006). There are several suggestions for the cause of the shallow decay phase, including energy injection into the afterglow shock (of two main types), viewing angles slightly outside the region of bright afterglow emission (see Figure 7), a complex angular structure of the jet consist-

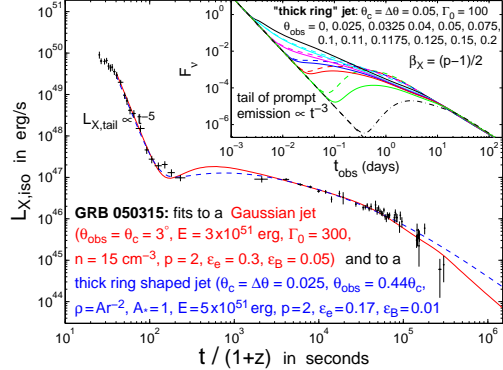


Fig. 7. A tentative fit to the X-ray light curve of GRB 050315, with (i) a Gaussian jet (solid red line), and (ii) a ring shaped (or hollow cone) jet, uniform within $\theta_c < \theta < \theta_c + \Delta\theta$ (blue dashed line) where in both cases the viewing angle plays a major role in producing the shallow decay phase (from Eichler & Granot, 2006). The initial fast decay is attributed to the tail of the prompt emission and modeled as a power law $\propto t^{-5}$. The inset shows afterglow light curves for a ring shaped jet (Granot, 2005), for different viewing angles θ_{obs} from the jet symmetry axis.

ing of two or more components (see Figure 8), and time varying shock microphysics parameters (for a review see Granot, 2007b). Nevertheless, it is not clear which of these, if any, is indeed the dominant cause.

The shallow decay phase has interesting implications for GRB and afterglow theory. It implies a very high efficiency ($\gtrsim 90\%$) of the prompt γ -ray emission, unless either the energy in the afterglow shock at late times ($\gtrsim 10$ hr) has been underestimated, or the shock microphysics parameters significantly vary with time during the early afterglow (Granot, Königl & Piran, 2006). Both are required in order for the γ -ray efficiency to be $\lesssim 10\%$,

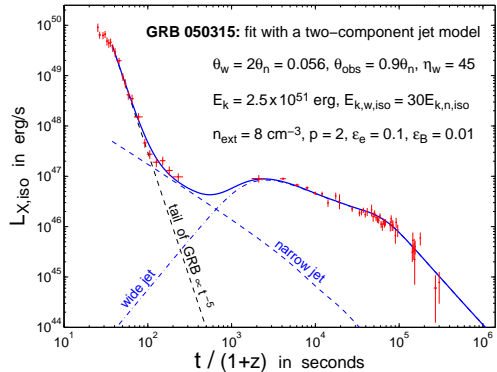


Fig. 8. Tentative fit to the X-ray light curve of GRB 050315 with the two-component jet model (from Granot, Königl & Piran, 2006). In addition to the total light curve (*thick solid line*) also shown are the separate contributions of the different components: the tail of the prompt emission ($\propto t^{-5}$), the narrow outflow, and the wide outflow. Here $E_k = E_{k,w} + E_{k,n}$ is the total kinetic energy of the two components. The narrow and wide components occupy the non-overlapping ranges in the polar angle θ (measured from the symmetry axis): $\theta < \theta_n$ and $\theta_n < \theta < \theta_w$, respectively; θ_{obs} is the viewing angle with respect to the jet symmetry axis.

which the internal shocks model can reasonably produce. This in turn requires a large energy in the afterglow shock (typically $\gtrsim 10^{52}$ erg). Nevertheless, it can still be accommodated within the framework of the standard afterglow model, albeit, with some modifications.

Another interesting finding by *Swift* is that the early optical emission, which has been attributed in some cases before *Swift* to the reverse shock, is typically much dimmer than expected (Roming et al., 2006). This may be since the expectations were too high (Nakar & Piran, 2004) and

motivated by early pre-*Swift* detections that were exceptionally bright. Alternatively, it could be (at least partly) due to a suppression of the reverse shock in strongly magnetized GRB outflows (Zhang & Kobayashi, 2005), or since *Swift* detects dimmer events (on average) compared to previous instruments, due to its higher sensitivity. The latter may also partly explain the relative paucity of detected jet breaks in the *Swift* era (Burrows & Racusin, 2007; Sato et al., 2007; Kocevski & Butler, 2008), although it is not clear yet if this can account for all of the effect.

5 Crisis, Ideas for Solving it, and Future Prospects

Among the new observational features in the *Swift* era, the most difficult one to naturally explain within the framework of the standard afterglow model is chromatic breaks in the afterglow light curves. Several GRBs show this feature, where the X-rays show a clear break (steepening of the flux decay rate) while the optical does not (e.g., Panaitescu et al., 2006, see Figure 9). The break in the X-ray light curve is usually identified with the end of the shallow decay stage. The optical light curve follows a single power law decay, usually with a temporal decay index intermediate between those in the X-rays before and after the break. Such chromatic breaks appear to be common among the best monitored *Swift* afterglows. Explaining these chromatic breaks requires significant changes to the

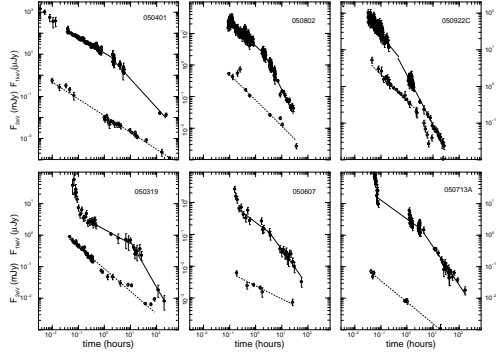


Fig. 9. Light-curves of six Swift GRB afterglows showing a chromatic X-ray break that is not seen in the optical at the same time (from Panaitescu et al., 2006). Optical data are shown with open symbols and are fit with a power-law decay (*dotted lines*); X-ray data are shown with filled symbols and fit with a broken power-law (*solid lines*).

existing afterglow model. This marks a crisis for standard afterglow theory.

Accommodating such chromatic breaks in a model where the X-ray and optical emissions arise from the same physical region (e.g., Panaitescu et al., 2006) requires not only time dependent microphysical parameters, but also fine tuning their time (or shock Lorentz factor) dependence in such a way that will produce a break in the X-ray but not in the optical, which appears somewhat contrived. The X-ray and optical may arise in separate physical components, which would naturally account for their seemingly decoupled light curves. However, this type of explanation also introduces a new ingredient (with its associated degrees of freedom) into the model, and unless it can be tested against other independent data it is hard to constrain such an option or reach any definitive conclusions. One might

ask: are we just adding epicycles to a fundamentally flawed model?

This crisis has led several people to consider more radical solutions. A good example, is the possibility that the afterglow is dominated by emission from a long-lived reverse shock, as opposed to emission from the forward shock as in the standard afterglow model (Genet, Daigne & Mochkovitch, 2007; Uhm & Beloborodov, 2007). This has the advantages of avoiding the need to produce near equipartition values of the shock microphysics parameters ($\epsilon_B \gtrsim 0.01$ and $\epsilon_e \gtrsim 0.1$) in the forward shock (which appears to be difficult, and relies on the poorly understood physics of relativistic collisionless shocks) and reducing the required efficiency of the prompt γ -ray emission. On the other hand, it has its own difficulties, such as tending to over-produce the observed optical emission (when normalized to the observed X-ray flux), and a self-absorption frequency that is typically above the radio band (which is hard to reconcile with radio afterglow detections, although these are admittedly rare in the *Swift* era).

Moreover, if taken to the extreme, where the emission is dominated by the reverse shock up to very late times (Uhm & Beloborodov, 2007), then the following problem arises. In a few cases the radio afterglows are observed out to very late times when the flow becomes sub-relativistic (e.g., Pihlström et al., 2007) with no apparent transition from being dominated by one component (the reverse shock) to another (the forward

shock). In the Newtonian regime, however, the properties of GRB remnants should approach those of supernova remnants, which are often directly resolved with the radio emission being dominated by the forward shock.

Another rather radical suggestion is that the X-ray emission from the onset of the shallow decay phase and onwards is dominated by “late prompt” emission (Ghisellini et al., 2007), due to prolonged activity of the central source, while the optical emission during the same time is dominated by the forward shock emission (i.e. the traditional afterglow emission). Since the X-ray and optical emissions in this model come from distinct physical regions, they are naturally decoupled. What appears to be less natural, however, is that both the prompt emission and the “late prompt” emission arise from similar activity of the central source but have very different temporal (very variable versus smooth) and spectral properties. Furthermore, this scenario requires an even higher efficiency of the prompt γ -ray emission, since the X-ray afterglow flux in this model is below the observed X-ray flux, implying a smaller energy in the afterglow shock. It also requires cold acceleration (not driven by thermal pressure) since after the break in the X-rays the flow Lorentz factor exceeds the inverse of its half-opening angle.

In summary, as the afterglow observations improve, a more complex behavior is revealed, which requires the introduction of new ingredients

into the model. Furthermore, some of the basic underlying physics, such as a detailed study of relativistic collisionless shocks and the dynamics of GRB jets, are still not fully understood and require further work. Out of the new observations in the *Swift* era, the most puzzling for afterglow theory are the shallow decay phase and the chromatic breaks. The former has too many possible explanations, and it is hard to tell which of them if any is indeed the dominant cause, while the latter is still awaiting a natural and convincing explanation without any major problems. These new observations challenge traditional afterglow theory and call for new ideas.

Broad band multi-frequency observations can help constrain the cause of the shallow decay phase (e.g. distinguish between a highly relativistic and mildly relativistic long lived reverse shock in the energy injection scenario) and chromatic breaks in GRB afterglows. Such observations may also help study the cause of the chromatic breaks. In particular, observations with the Large Area Telescope (LAT) on board the Gamma-ray Large Area Space Telescope (GLAST, to be launched in early 2008) may give us a better handle on the SSC component which would provide more constraints on the model, and help distinguish between different scenarios.

The author gratefully acknowledges a Royal Society Wolfson Research Merit Award.

References

- Akerlof, C., et al. 1999, *Nature*, 398, 400
- Bersier, D., et al. 2003, *ApJ*, 584, L43
- Blandford, R. D., & McKee, C. F. 1976, *Phys. Fluids*, 19, 1130
- Böttcher, M., & Dermer, C. D. 2000, *ApJ*, 532, 281
- Burrows, D. N., et al. 2005, *Science*, 309, 1833
- Burrows, D. N., & Racusin, J. 2007, preprint (astro-ph/0702633)
- Cannizzo, J. K., Gehrels, N., & Vishniac, E. T. 2004, *ApJ*, 601, 380
- Chevalier, R. A., & Li, Z.-Y. 1999, *ApJ*, 520, L29
- Cohen, E., Piran, T., & Sari, R. 1998, *ApJ*, 509, 717
- Costa, E., et al. 1997, *Nature*, 387, 783
- Covino, S., et al. 1999, *A&A*, 348, L1
- Covino, S., et al. 2003, *A&A*, 400, L9
- Eichler, D., & Granot, J. 2006, *ApJ*, 641, L5
- Fox, D. W., et al. 2003, *Nature*, 422, 284
- Frail, D. A., et al. 1997, *Nature*, 389, 261
- Galama, T. J., et al. 1998, *ApJ*, 500, L97
- Garnavich, P. M., Loeb, A., & Stanek, K. Z. 2000, *ApJ*, 544, L11
- Gaudi, B. S., Granot, J., & Loeb, A. 2001, *ApJ*, 561, 178
- Genet, F., Daigne, F., & Mochkovitch, R. 2007, *MNRAS*, 381, 732
- Ghisellini, G., Ghirlanda, G., Nava, L., & Firmani, C. 2007, *ApJ*, 657, 359
- Giannios, D. 2006, *A&A*, 455, L5
- Gorosabel, J., et al. 2006, *ApJ*, 641, L13
- Granot, J. 2005, *ApJ*, 631, 1022
- Granot, J. 2007a, in “Triggering Relativistic Jets”, Eds. W. H. Lee & E. Ramirez-Ruiz, *Rev. Mex. A&A*, 27, 140
- Granot, J. 2007b, *Il Nuovo Cimento B*, 121, 1073
- Granot, J., Miller, M., Piran, T., Suen, W. M., & Hughes, P. A. 2001, in “GRBs in the Afterglow Era”, ed. E. Costa, F. Frontera, & J. Hjorth (Berlin: Springer), 312
- Granot, J., Königl, A., & Piran, T. 2006, *MNRAS*, 370, 1946
- Granot, J., Nakar, E., & Piran, T. 2003, *Nature*, 426, 138
- Granot, J., Ramirez-Ruiz, E., & Loeb, A. 2005, *ApJ*, 618, 413
- Granot, J., & Sari, R. 2002, *ApJ*, 568, 820
- Gruzinov, A. 2007, preprint (astro-ph/0704.3081)
- Harrison, F. A., et al. 2001, *ApJ*, 559, 123
- Heyl, J. S., & Perna, R. 2003, *ApJ*, 586, L13
- Katz, J. I. 1994, *ApJ*, 422, 248
- Keshet, U., & Waxman, E. 2005, *Phys. Rev. Lett.*, 94, 1102
- Kocevski, D., & Butler, N. 2008, *ApJ*, 680, 531
- Krimm, H. A., Granot, J., et al. 2007, *ApJ*, 665, 554
- Kulkarni, S. R., et al. 1999, *ApJ*, 522, L97
- Kumar, P., & Granot, J. 2003, *ApJ*, 591, 1075
- Kumar, P., & Panaitescu, A. 2000, *ApJ*, 541, L51
- Kumar, P., & Piran, T. 2000a, *ApJ*, 532, 286
- Kumar, P., & Piran, T. 2000b, *ApJ*, 535, 152
- Laursen, L. T., & Stanek, K. Z. 2003, *ApJ*, 597, L107
- Lazzati, D., et al. 2002, *A&A*, 396, L5

- Lipkin, Y. M., Ofek, E. O., Gal-Yam, A., et al. 2004, *ApJ*, 606, 381
- Lyubarsky, Y., & Eichler, D. 2006, *ApJ*, 647, 1250
- Medvedev, M. V., & Loeb, A. 1999, *ApJ*, 526, 697
- Mészáros, P. 2006, *Rept. Prog. Phys.*, 69, 2259
- Mészáros, P., & Rees, M. J. 1997, *ApJ*, 476, 232
- Mészáros, P., & Rees, M. J. 1999, *MNRAS*, 306, L39
- Nakar, E., & Granot, J. 2007, *MNRAS*, 380, 1744
- Nakar, E., Piran, T., & Granot, J. 2003, *New Astron.*, 8, 495
- Nakar, E., & Oren, Y. 2004, *ApJ*, 602, L97
- Nakar, E., & Piran, T. 2003, *ApJ*, 598, 400
- Nakar, E., & Piran, T. 2004, *MNRAS*, 353, 647
- Nousek, J. A., et al. 2006, *ApJ*, 642, 389
- O'Brien P., et al. 2006, *ApJ*, 647, 1213
- Oren, Y., Nakar, E., & Piran, T. 2004, *MNRAS*, 353, L35
- Paczynski, B., & Rhoads, J. 1993, *ApJ*, 418, L5
- Panaitecu, A., et al. 2006, *MNRAS*, 369, 2059
- Pandey, S. B., et al. 2002, *Bull. Astron. Soc. India*, 31, 19
- Pihlström, Y. M., Taylor, G. B., Granot, J., & Doeleman, S. 2007, *ApJ*, 664, 411
- Piran, T. 2005, *Rev. Mod. Phys.*, 76, 1143
- Ramirez-Ruiz, E., Merloni, A., & Rees, M. J. 2001, *MNRAS*, 324, 1147
- Rees, M. J., & Mészáros, P. 1998, *ApJ*, 496, L1
- Rhoads, J. E. 1997, *ApJ*, 487, L1
- Rhoads, J. E. 1999, *ApJ*, 525, 737
- Rol, E. et al. 2000, *ApJ*, 544, 707
- Roming, P. W. A., et al. 2006, *ApJ*, 652, 1416
- Sari, R., & Esin, A. A. 2001, *ApJ*, 548, 787
- Sari, R., & Mészáros, P. 2000, *ApJ*, 535, L33
- Sari, R., & Piran, T., 1995, *ApJ*, 455, L143
- Sari, R., & Piran, T., 1997, *ApJ*, 485, 270
- Sari, R., & Piran, T., 1999a, *ApJ*, 520, 641
- Sari, R., & Piran, T., 1999b, *ApJ*, 517, L109
- Sari, R., & Piran, T., & Halpern, J. P. 1999, *ApJ*, 519, L17
- Sato, G., et al. 2007, *ApJ*, 657, 359
- Spitkovsky, A. 2008, *ApJ*, 673, L39
- Stanek, K. Z., et al. 1999, *ApJ*, 522, L39
- Taylor, G. B., Frail, D. A., Berger, E., & Kulkarni, S. R. 2004, *ApJ*, 609, L1
- Taylor, G. B., Momjian, E., Pihlström, Y., Ghosh, T., & Salter, C. 2005, *ApJ*, 622, 986
- Uhm, Z. L., & Beloborodov, A. M. 2007, *ApJ*, 665, L93
- van Paradijs, J., et al. 1997, *Nature*, 386, 686
- Vaughan, S., et al. 2006, *ApJ*, 638, 920
- Wang, X., & Loeb, A. 2000, *ApJ*, 535, 788
- Waxman, E. 1997, *ApJ*, 485, L5
- Waxman, E., Kulkarni, S. R., & Frail, D. A. 1998, *ApJ*, 497, 288
- Wijers, R., Rees, M. J., & Mészáros, P. 1997, *MNRAS*, 288, L51
- Wijers, R. A. M. J., et al. 1999, *ApJ*, 523, L33
- Zhang, B., & Kobayashi, S. 2005, *ApJ*, 628, 315